FRACTIONATION OF THE NUCLEUS BY DIVALENT CATIONS

Isolation of Nuclear Membranes

ARIANE MONNERON, GÜNTER BLOBEL, and GEORGE E. PALADE

From The Rockefeller University, New York 10021

ABSTRACT

0.3–0.5 M $MgCl_2$ was used to disassemble nuclei and to isolate by a single centrifugation in less than 3 hr a nuclear envelope fraction in 55–60% yield as assessed by phospholipid recovery. Its gross chemical composition was determined and its morphology was studied electron microscopically by sectioning, freeze etching, and negative staining procedures.

INTRODUCTION

Available procedures for the subfractionation of the nucleus involve disruption of isolated nuclei by physical (e.g., hypotonic shock, sonication) or chemical (e.g., salts, acids, detergents, enzymes) means, or a combination of both, followed by various centrifugation schemes, the usual objective being the isolation of a single subnuclear component. For instance, published techniques (1–5) for the isolation of the nuclear envelope rely on: (*a*) the disruption of isolated nuclei by either a combination of sonication and high concentrations of salt (potassium citrate [1], potassium chloride [2]), or (*b*) incubation with DNase followed by treatment with high concentrations of salt (sodium chloride [3], magnesium chloride [4]). Most of these procedures are relatively lengthy because they ask for long periods of incubation in DNase or salt, or because they require several centrifugation steps (2, 5). Furthermore, recovery of envelope membranes in terms of phospholipids, given only in two instances, is less than 50%: 24–36% (1) and 47.1% (4).

Since a wide range of electrostatic forces from weak to very strong is responsible for interactions among nucleic acids and proteins, and among various ribo- and deoxyribonucleoproteins, we wondered whether the entire organization of the nucleus, including the association of the nuclear envelope with adjacent nucleoproteins, does not depend primarily on such forces. Were this the case, electrolytes alone, without the disruption of structures by sonication or the degradation of macromolecules by enzymes, should be sufficient for our objective which is a stepwise disassembly of the nucleus, and a subsequent balance sheet-oriented fractionation.

We have put this assumption to test and in this paper we show that a nuclear envelope fraction of recognizable morphology can be isolated in high yield and purity by a short, one-step centrifugation from rat liver nuclei treated with high concentrations of divalent cations.

METHODS

A. Isolation of Nuclear and Microsomal Fractions

Nuclear and rough microsomal fractions were prepared from rat liver homogenates (1:2, w:v, in 0.25 M sucrose-TKM), as previously described (6–8), except

that the procedure for the preparation of the nuclear fraction was adapted to larger amounts of tissue by using the Spinco SW 25 rotor (Beckman Instrument, Inc., Spinco Div., Palo Alto, Calif.) and by centrifuging for 2 hr at 25,000 rpm. The yield of nuclei as measured by DNA recovery was ~ 70%. The isolated nuclei (not subjected to detergent as in reference 6) were resuspended in cold 0.25 M sucrose-TKM (0.05 M Tris-HCl, pH 7.5,[1] 0.025 M KCl, 0.005 M $MgCl_2$) and centrifuged for 10 min at 1000 $g_{(avg)}$ to remove a few remaining contaminants, primarily collagen fibrils. The pellet of washed nuclei was gently stirred with a spatula in twice its volume of glycerol and stored at − 20°C.

B. Preparation of Nuclear Envelopes

All operations were performed near 0°C. To estimate and adjust the approximate concentration of nuclei, we determined the A_{260} of the glycerol suspension and then diluted it with ice-cold 0.25 M sucrose-TKM until a concentration of ~ 30 A_{260} units per ml was reached. 5-ml samples of the diluted suspension were then transferred to tubes fitting the SB 283 rotor of the IEC centrifuge (International Equipment Co., Needham Heights, Mass.) and the nuclei were quantitatively pelleted by a 5 min centrifugation at ~ 1000 $g_{(avg)}$. Each tube used for subsequent fractionation contained, therefore, the same amount of nuclei: ~ 150 A_{260} units. Each pellet was stirred with a spatula in 2–3 drops of glycerol to facilitate the following resuspension in 1.8 ml of a solution which was 1.8 M in sucrose, 0.5 M in $MgCl_2$, and 0.05 M in Tris-HCl, pH 7.5. This step resulted in an extremely viscuous but homogeneous suspension (if glycerol was omitted, small clumps were noticed), which was briefly and vigorously vortexed three times at 5 min intervals. A brief centrifugation (5 min at 1000 *g*) collected the material adhering to the tube wall and floated air bubbles on top into a thin foamy layer, which was removed with a spatula. A linear ~ 10.5 ml gradient of 20%–55% sucrose in 0.5 M $MgCl_2$ and 0.05 M Tris-HCl, pH 7.5, was generated on top of the 2 ml load zone which contained the treated nuclear suspension. The gradients were centrifuged for 2 hr at 40,000 rpm (190,000 $g_{(avg)}$) in the SB 283 rotor of the IEC centrifuge.

The optical density of the developed gradients was monitored continuously at 260 or at 440 nm, and each gradient was divided into 12 fractions of 1 ml, which were collected from the top using the Buchler Auto-Densiflow (Buchler Instruments, Inc., Fort Lee, N. J.) connected to a peristaltic pump. A thin glassy pellet and less than 0.5 ml liquid remained at the bottom of each tube.[2]

For comparison, an isolated rough microsomal fraction (8) was resuspended in 1.8 M sucrose-0.5 M $MgCl_2$-0.05 M Tris HCl, pH 7.5, and floated under the same conditions.

Nuclear envelope fractions were also prepared from nuclei extracted with other divalent (Ca^{2+}, Mn^{2+}) or monovalent (K^+) cations. To this intent, the $MgCl_2$ in the extraction medium was replaced by either 0.5 M $CaCl_2$ or $MnCl_2$ or KCl at the same concentration (in the case of KCl, 5 mM $MgCl_2$ was also present), the rest of the procedure being as indicated above, except that for the KCl extract a longer centrifugation was needed to develop the gradients (see Results).

C. Chemical Determination

To put the data in balance sheet form, a sample of the original suspension of nuclei (~ 30 A_{260} units/ml) and all fractions collected from the developed gradient, including the pellet, were analyzed. To this intent the equivalent of 1 ml fractions and the pellets from six gradients were pooled for each experiment and 1 ml samples from each pool were used to determine the amount of protein, phospholipid, RNA, and DNA in the corresponding fraction.

Protein was measured according to Lowry et al. (9) after one precipitation with 10% trichloroacetic acid (TCA). Bovine serum albumin, treated identically, was used as a standard.

Lipids were extracted from the 10% TCA precipitate by the procedure of Folch et al. (10). The lipid phosphorus was determined according to Ames and Dubin (11) and the values found were converted to phospholipid by multiplying by 25.

RNA was measured by a modified Schmidt-Tannhauser procedure as described in (12), and DNA was determined according to Burton and Peterson (13), using deoxyadenosine as a standard.

D. SDS-Gel Electrophoresis

The dissolution of the polypeptide chains of the nuclear envelope and rough microsomes and their separation by electrophoresis were performed essentially as described by Maizel (14), using 7.5% acrylamide-sodium dodecyl sulfate (SDS) gels and the E-C apparatus (E-C Apparatus Corp., Philadelphia, Pa.) with a 3 mm thick slab provided with eight slots. After electrophoresis, the gels were stained in Coomassie brilliant blue.

[1] At 20°C.

[2] Examination of the translucent pellet at the bottom of the tube has shown that it mainly consists of nucleoli which retain their intranuclear size and shape, but in which a distinction between the granular and fibrillar parts is no longer apparent.

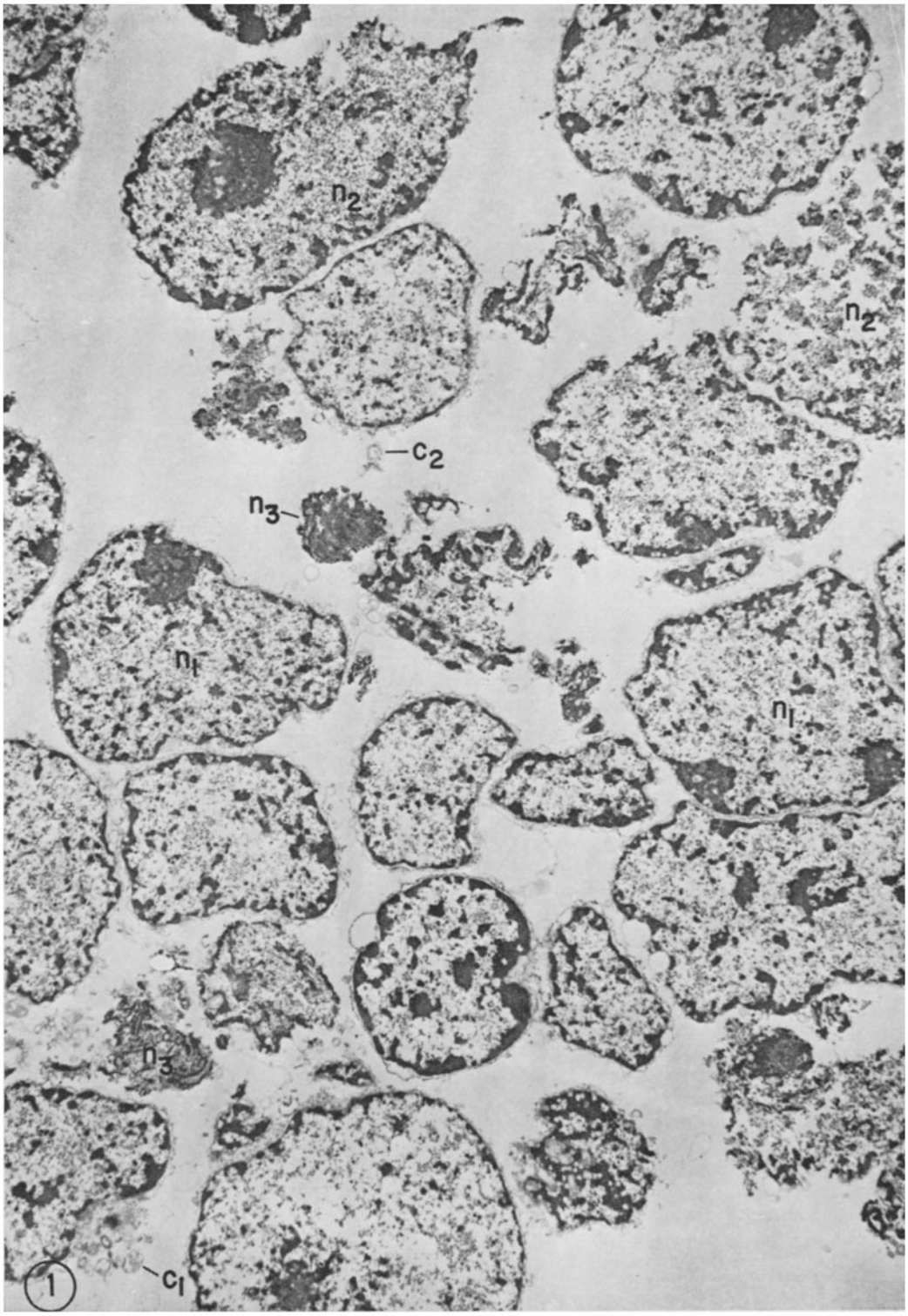

FIGURE 1 Section through a nuclear fraction pellet. The fraction consists of apparently intact nuclei (n_1) sectioned at different levels, partly ruptured nuclei (n_2), and nuclear fragments (n_3). For structural details of the nuclei and their envelope see Fig. 2. The fraction contains few cytoplasmic contaminants in the form of tabs attached to nuclei (c_1), or of apparently isolated particles (c_2). × 5100.

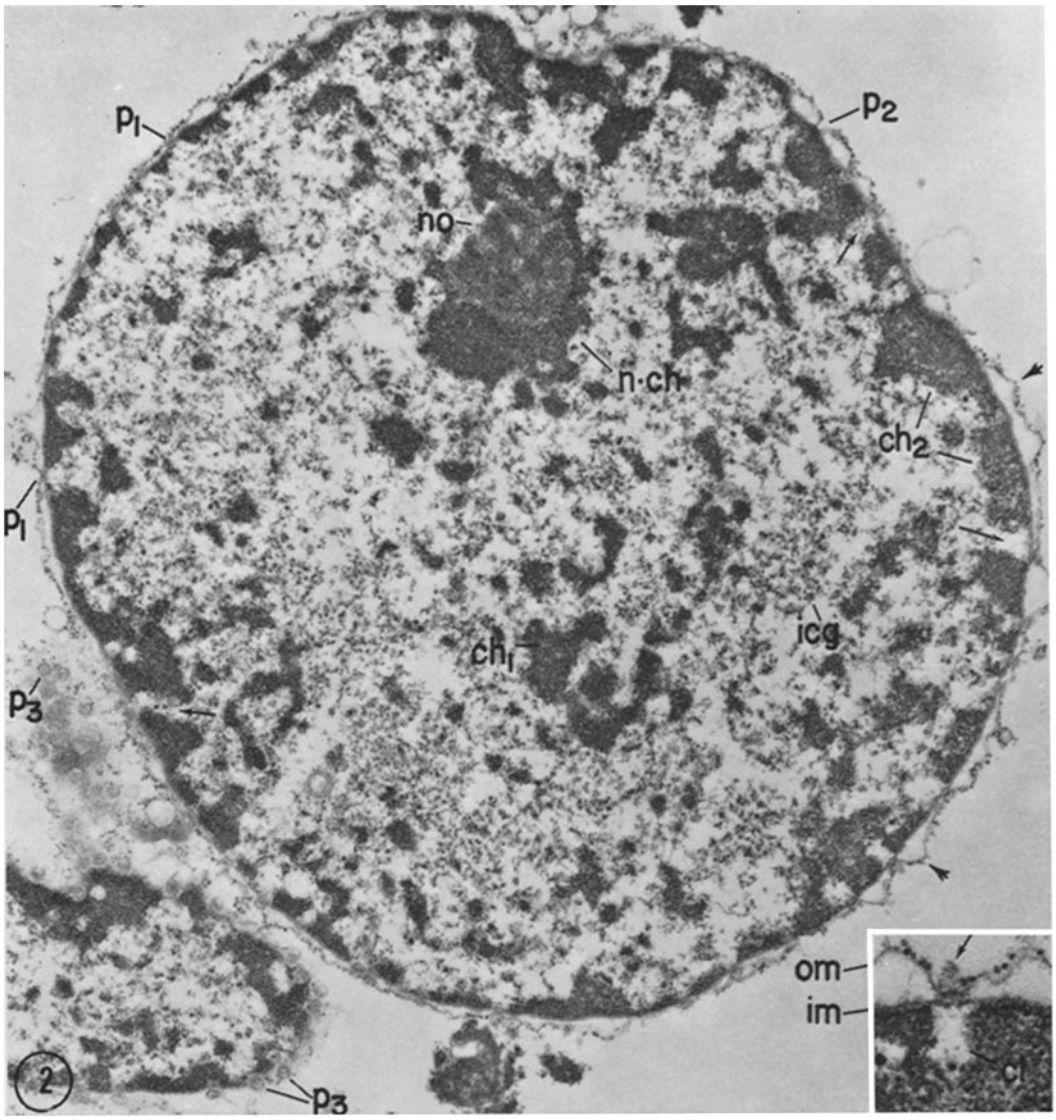

FIGURE 2 Higher magnification of an isolated nucleus from a nuclear fraction similar to the one in Fig. 1. The micrograph shows the extent to which the organization of the nucleus is preserved during the isolation procedure. The structure of the nucleolus (*no*) with its associated chromatin (*n·ch*), the central (ch_1), and peripheral (ch_2) condensed chromatin masses, the channels leading through the peripheral chromatin to the nuclear pores (arrows), and the interchromatin granules (*icg*) are similar to the corresponding structures seen in hepatocyte nuclei *in situ*. The same applies to the nuclear envelope, except that the space of the perinuclear cisterna shows many focal dilations (arrowheads). Nuclear pores, most of them provided with plugs (p_1), are seen around the entire perimeter. A plug-free pore is marked p_2. The grazing section of an adjacent nucleus shows full-faced images of nuclear pores at p_3. The *inset* illustrates the appearance of a plugged pore in normal section. The ribosome-bearing outer membrane is marked *om*, the inner membrane *im*, and the intrachromatin channel leading to the pore, *cl*. The arrow points to the pore plug. × 11,500; *inset*, × 26,000.

E. Electron Microscopy

(1) SECTIONED MATERIAL: Nuclear pellets, pellets recovered from salt-treated nuclear suspensions, and pellets collected at the bottom of the sucrose gradients were fixed for 1 hr at 4°C in 1.8% glutaraldehyde in buffer, postfixed for 1 hr at ~25°C in 1% OsO_4 in the same buffer, dehydrated in ethanol, and embedded in Epon (15).

For nuclear envelope fractions, the band seen in the developed gradient was collected, diluted with the same salt-buffer solution as used in the gradient, and centrifuged for 1 hr at 78,500 $g_{(avg)}$. The ensuing pellets were fixed in either 2% OsO_4 in acetate Veronal buffer or in 1.5% buffered glutaraldehyde followed by 2% OsO_4 in water, or finally in 1.8% glutaraldehyde in 0.5 M $MgCl_2$. The latter mixture was used to check the possible effects of hypotonic shock during fixation. Some of the pellets were stained in block in 0.5% uranyl acetate in acetate Veronal buffer before dehydration and Epon embedding (16).

Sections cut with diamond knives on MT2 Sorvall microtomes (Ivan Sorvall, Inc., Norwalk, Conn.) were stained with uranyl acetate (17) and lead citrate (18).

(2) NEGATIVE STAINING: Small samples of the material in the band were negatively stained with 2% ammonium molybdate without prior fixation.

(3) FREEZE CLEAVAGE: Nuclear fractions resuspended in 20% glycerol and nuclear envelope fractions similarly treated were frozen in liquid Freon 22 cooled to liquid nitrogen temperature (−195°C). The preparations were fractured at −100°C in a Balzer Machine (Balzer High Vacuum Corp., Santa Ana, Calif.), shadowed with carbon-platinum, and replicated with carbon. The replicas were prepared for electron microscopy by current procedures (19).

All the preparations were examined in a Siemens 101 Elmiskop or a Hitachi 11C microscope, operated at 80 and 75 kv, respectively, with 50-μ objective apertures and 200-μ condenser apertures, and calibrated with a cross-lined grating replica (2160 lines/mm).

RESULTS

A. Morphology of Starting Preparations

(1) SECTIONED SPECIMENS

In confirmation of previous observations (6, see also 22), the nuclear fraction isolated and washed as described under Methods consists almost entirely of nuclei, primarily hepatocyte nuclei (Fig. 1), with little contamination by Kupffer cell fragments, collagen fibrils, and very rarely by mitochondria. Micrographs at appropriate magnifications (Fig. 2) show that the structural features recognized in nuclei *in situ* (i.e., the nucleoli, the dense chromatin, and the interchromatin gran-

FIGURE 3 Freeze-cleaved preparation of a nuclear fraction similar to the one in Fig. 1. In all cases the direction of shadowing on the replicas is indicated by a heavy arrow. Fig. 3 *o* shows the two membranes of the nuclear envelope seen from outside, and Fig. 3 *i* shows the same membranes seen from inside. In Fig. 3 *o*, *A* marks the face of the inner leaflet of the outer membrane. The appearance of its plugged pores, reminiscent of that of a circumvallate papilla, is seen in detail in the enlarged *inset* A. The complementary face *B*, i.e., the outer leaflet of the outer membrane seen from inside, appears on Fig. 3 *i* (*B*) and Fig. 3 *o* (*B*); note that it has a higher frequency of small particles than face *A*, and that on this face the pores take the appearance of deep craters, suggesting that upon cleavage the plugs are generally removed with the inner leaflet. A higher magnification of a pore crater characteristic of this face is shown in *inset* B. In a few cases, the craters are replaced by protruding mounds (Fig. 3 *o*, *B*, m_o) suggesting that occasionally the plugs remains with the outer leaflet upon cleavage of the outer membrane. The inner leaflet of the inner membrane as seen from outside appears in Fig. 3 *o* at *D*. It is characterized by a high population of small (100-80 A) particles, some of them disposed in rows, and by crater-like pores, details of which are shown at higher magnification in *inset* D. Only occasionally the craters are replaced by mounds (m_i). Finally, the outer leaflet of the inner membrane, seen from inside, appears in Figs. 3 *i* and 3 *o* at *C*. This face has a smaller and more heterogeneous population of small particles and the pores appear on it like circumvallate papillae, frequently provided with long whiskers. These details are shown at higher magnification in *inset* C. Note in the *insets* the rather pronounced polygonal outline of the pores; most of them appear to be octagonal (cf. 25, 30). Steps up along the irregular fracture plane are indicated by ↑ and steps down by ↓, irrespective of the general convexity or concavity of the surfaces. The fracture goes almost normally through the nuclear envelope and the nuclear content at *ne* and *nc*, respectively, in Fig. 3 *o*. Figs. 3 *o* and 3 *i* came from the same micrographs; 3 *i* has been translated by 36 mm to the right, as shown by the images of two small nuclear envelope blebs (b_1, b_2). 3 *o* and 3 *i*, × 45,000; all *insets*, × 150,000.

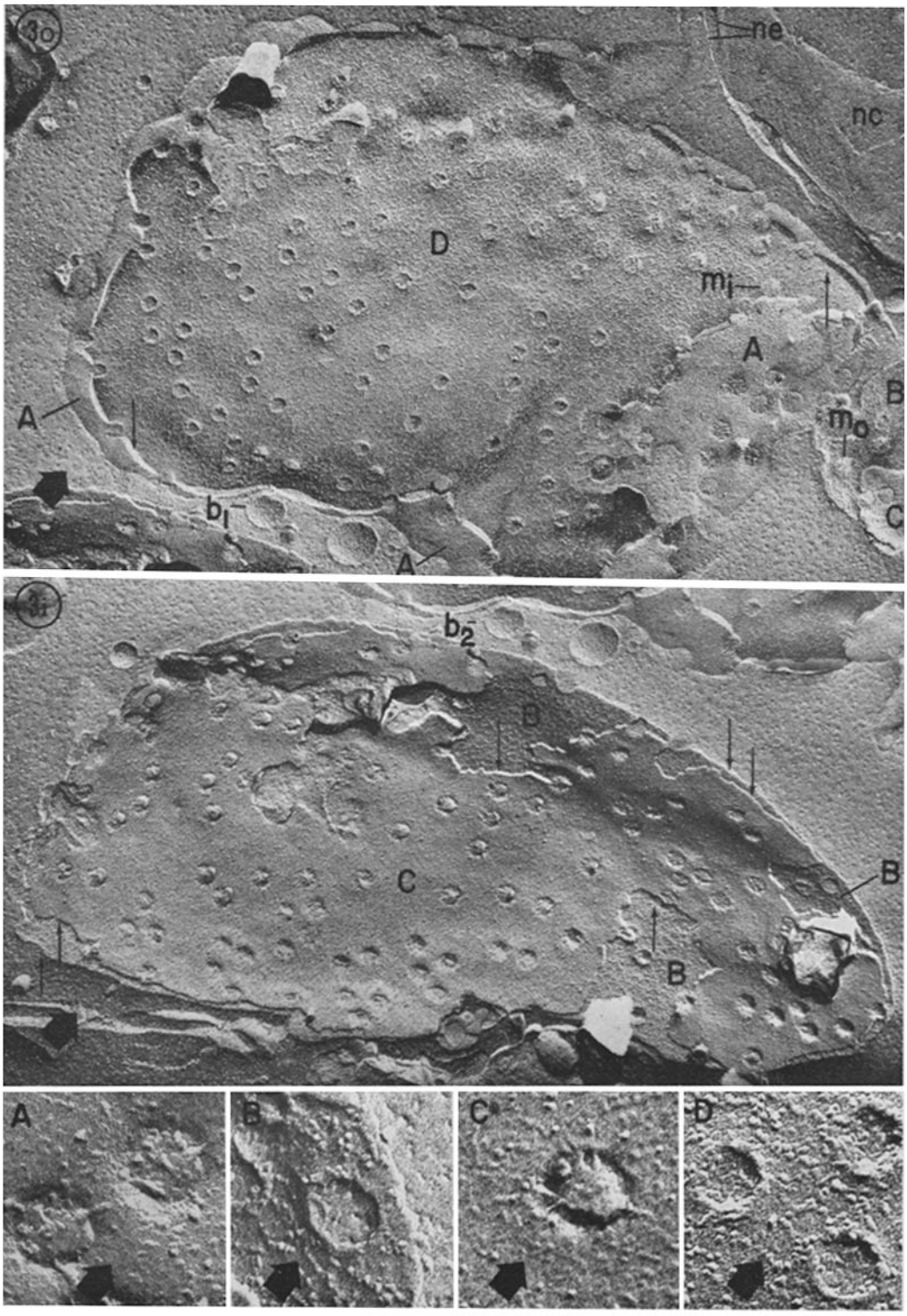
3o
ne
nc
D
m_i
A
B
m_o
C
A
b_1
A
3i
b_2
B
C
B
B
B
A
B
C
D

ules) are retained unchanged throughout the isolation procedure.

More important for the aim of the present paper, a nuclear envelope with its two membranes, its pores and pore complexes ("pore plugs") and the ribosomes attached to the cytoplasmic surface of the outer membrane is present at the periphery of practically all nuclei. The outer membrane has a few small blebs and is occasionally ruptured; the inner membrane is usually intact, presumably because it is supported by a quasi-continuous layer of dense chromatin which is interrupted only by short cylindrical channels leading to the pores (Fig. 2). A relatively large percentage of the nuclei in the fraction are partly disrupted (Fig. 1), but this situation is not expected to interfere with the isolation of nuclear envelopes.

(2) Freeze-Cleaved Specimens

As already known, such specimens yield no information concerning the internal organization of the nucleus (20); they are primarily useful in studying cleavage faces in membranes (21). For the nuclear envelope, the four expected views (cf. 21, 23), shown diagramatically in Fig. 4 I, could be recognized without difficulty. The inner or cisternal leaflet of the outer membrane seen from the outside (face *A*) showed relatively few randomly distributed particles of 80 A diameter[3] (Fig. 3 *o*). On this leaflet, most of the pores appeared as sharp circular or polygonal depressions, ~ 880 A in diameter with a slightly protruding

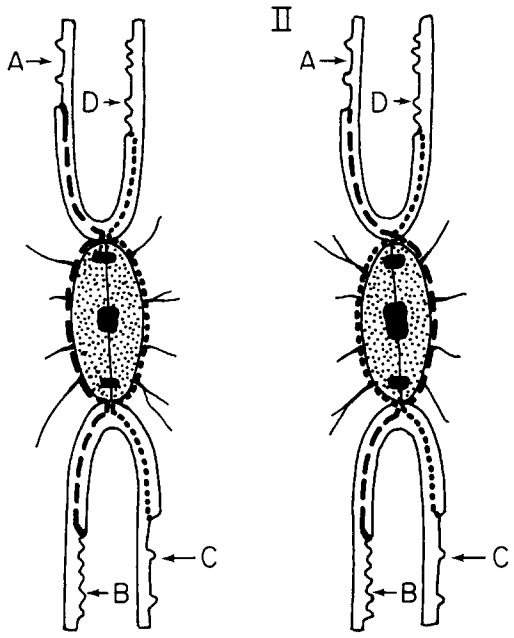

Figure 4 Diagrams to show the frequent (I) and occasional (II) path followed by fracture planes through the nuclear envelope pores.

bottom, an appearance reminiscent of a partly depressed, circumvallate papilla. The surface of the bottom was rather rough and from it, whiskers were seen protruding over the pore rims (Fig. 3 *o*, *A*). In some of the pores, the bottom protrusion was missing.

The outer or cytoplasmic leaflet of the outer membrane seen from inside (face *B*) showed a larger number of particles, and most of the pores appeared on it as circular or polygonal craters, ~ 800 A in diameter with a sharp protruding rim

[3] Most of these particles measure ~80 A; a few are as large as 100–110 A in diameter. The same relative distribution appears on the other cleavage surfaces.

Figure 5 Nuclear ghost in a nuclear fraction extracted with 0.5 M $MgCl_2$ in 0.05 M Tris-HCl buffer pH 7.4. The pellet obtained by centrifugation at 4°C for 2 hr at 190,000 $g_{(avg)}$ contained (from bottom to top) nucleoli, fibrillar masses, and large membrane sheets. Among the latter, were recognizable nuclear ghosts like the one (*g*) shown in this figure. The two membranes of the nuclear envelope (*om*, *im*) are easily identified as are the remnants of nuclear pore complexes (*p*) and of attached ribosomes (*r*). The nuclear content has been largely extracted probably through large ruptures like the one marked *t*. Only fine fibrils (*ch*) (dispersed chromatin?) and a few clusters of interchromatin granules (*icg*) remain within the ghosts. Some of the ghosts retain a nucleolus (not shown). × 27,000.

Figure 6 Nuclear fraction extracted with 0.5 M KCl in 0.005 M $MgCl_2$ and 0.05 M Tris-HCl buffer, pH 7.4. Suspension centrifuged and pellet processed and examined as for Fig. 5. The pellet shows no stratification and consists of large masses of apparently condensed chromatin (*ch*), unidentified dense aggregates (*x*), and clusters of vesicles (*v*) of varied sizes, some of them bearing attached ribosomes (*r*). × 21,000.

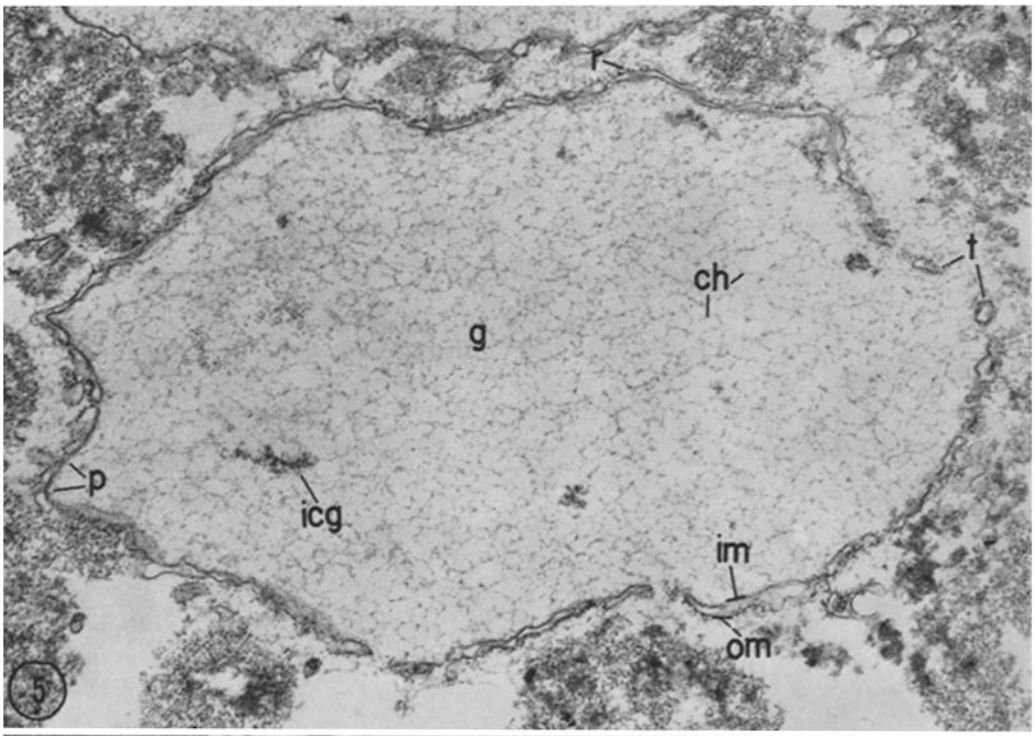
r
ch
t
g
p
icg
im
om
5

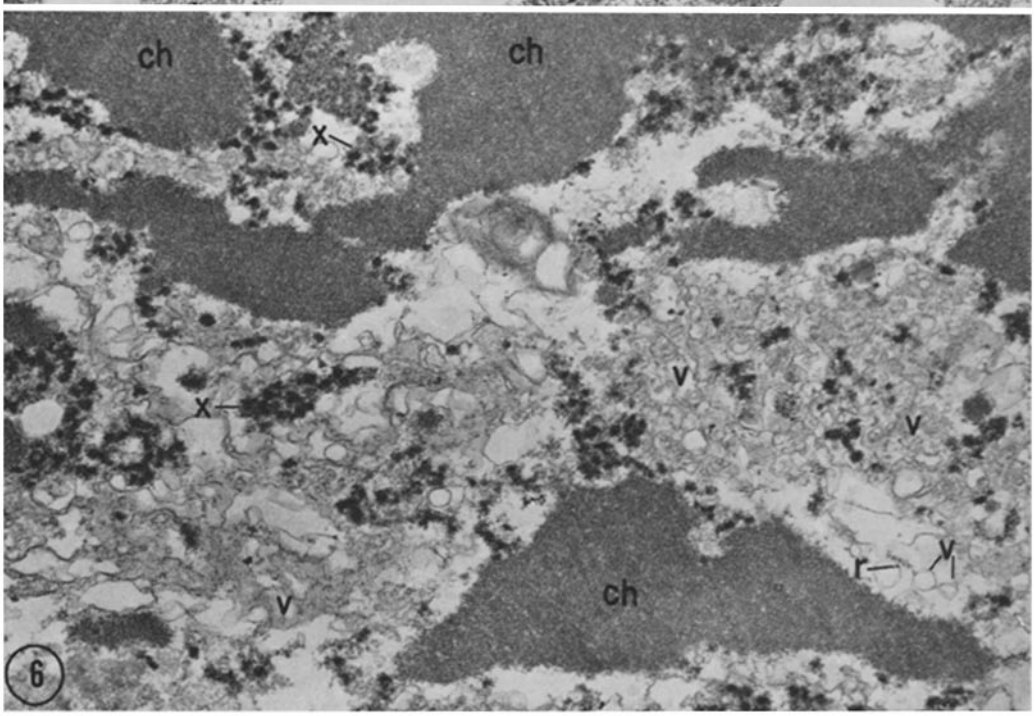
ch
ch
x
x
v
v
r
v
ch
v
6

and an evenly scooped bottom (Fig. 3 *i*, *B*); a few of them, however, looked like circular mounds with relatively rough tops (Fig. 3 *o*, m_o).

The appearance of the inner or nucleoplasmic leaflet of the inner membrane seen from outside (face *D*) was similar in that it showed a high frequency of craters and a low frequency of mounds at the site of the pores. The frequency of small (80–100 A) protruding particles was high (Fig. 3 *o*, *D*), and occasionally these particles were aligned in rows.

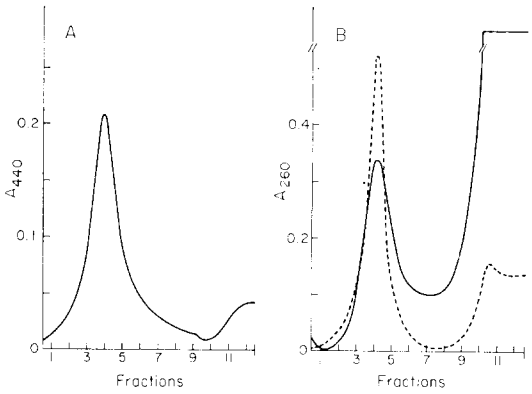

FIGURE 7 Gradient analysis of nuclei treated with 0.5 M $MgCl_2$. For details see Methods. Recording was at 440 nm (A) or 260 nm (B). Dotted line represents absorbancy profile at 260 nm of a membrane band collected from gradient, pelleted, and refloated.

Finally on the outer or cisternal leaflet of the inner membrane seen from inside (face *C*), the number of small particles was small and most of the pores again had an appearance reminiscent of depressed, circumvallate papillae with whiskers extending over the vallum and over the rims, while in a few the bottom protrusion was missing (Figs. 3 *i*-3 *o*, *C*). These various appearances could be explained by assuming that the pore plugs tend to remain behind with the rest of the envelope when either the innermost (nucleoplasmic) or outermost (cytoplasmic) leaflet of the envelope is cleaved away. Many of the features observed are similar to those recently described in freeze-cleaved preparations of lymphocyte and melanocyte nuclei *in situ* (24, 25). The two diagrams in Fig. 4

TABLE I

Distribution and Recovery of Nuclear Phospholipid, Protein, RNA, and DNA in Gradient Fractions

	Tube number												Pellet	Total (tubes 1–12 + pellet)	Input	Recovery	Recovery from 4 experiments
	1	2	3	4	5	6	7	8	9	10	11	12					
						μg							μg	μg	μg	%	%
PLP	10	21	36	109	43	18	8	10	9	9	41	29	15	357	405	88	94 ± 10
Protein	110	187	270	312	271	220	191	219	348	545	2136	3162	720	8691	7500	116	109 ± 11
RNA	2.3	1.9	9.1	13	14	10	8.8	7.7	7.5	36	207	238	44	599	586	102	102 ± 8
DNA	0.0	0.7	0.9	1.8	2.3	3.0	2.7	3.4	2.5	36	1130	1305	43	2531	2697	94	102 ± 8

For details see Methods. The fractions were collected from gradient corresponding to the solid line profile in Fig. 7 B. Values are from one experiment except for those in the last column, which are means from four experiments ± SE of the means.

FIGURE 8 Nuclear envelope fraction prepared from nuclei extracted with 0.5 M $MgCl_2$ in 0.05 M Tris-HCl buffer, pH 7.5. The nuclear envelope membranes were separated from the extract by floatation in a sucrose gradient as described under Methods and the ensuing band was diluted in the extraction medium and pelleted by centrifugation for 2 hr at 78,500 $g_{(avg)}$. The pellet was fixed with 2% OsO_4 in acetate Veronal buffer, pH 7.4, and stained in block with uranyl acetate before dehydration and embedding. This low magnification micrograph shows that the fraction is homogeneous: it consists of vesicles of different sizes which appear either dilated and seemingly empty (v_1), or dilated and containing tubular remnants (v_2), or small and relatively well packed (v_3). For further details see Fig. 9. The bottom of the pellet is marked *t*. × 5100.

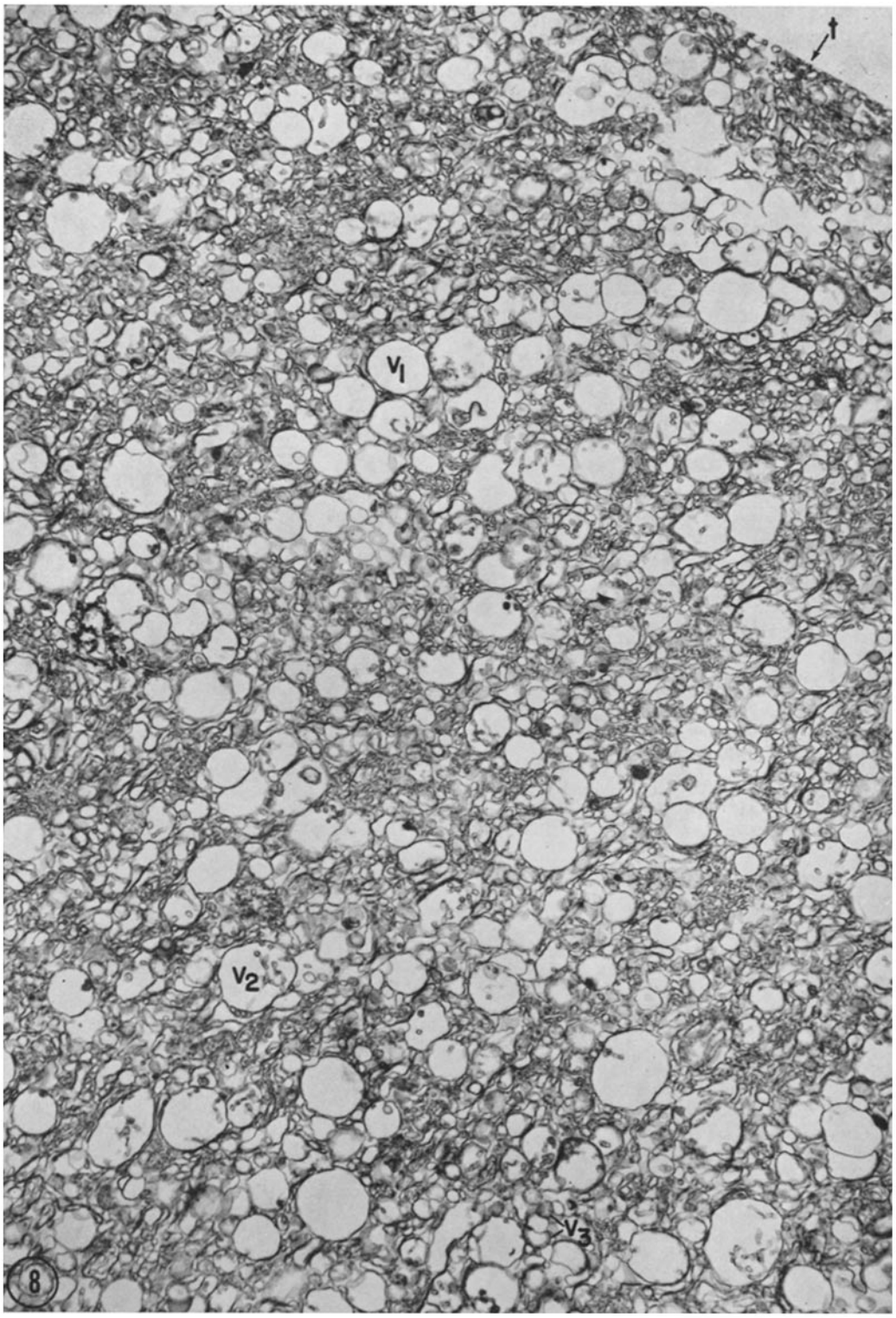
V1
V2
V3
8

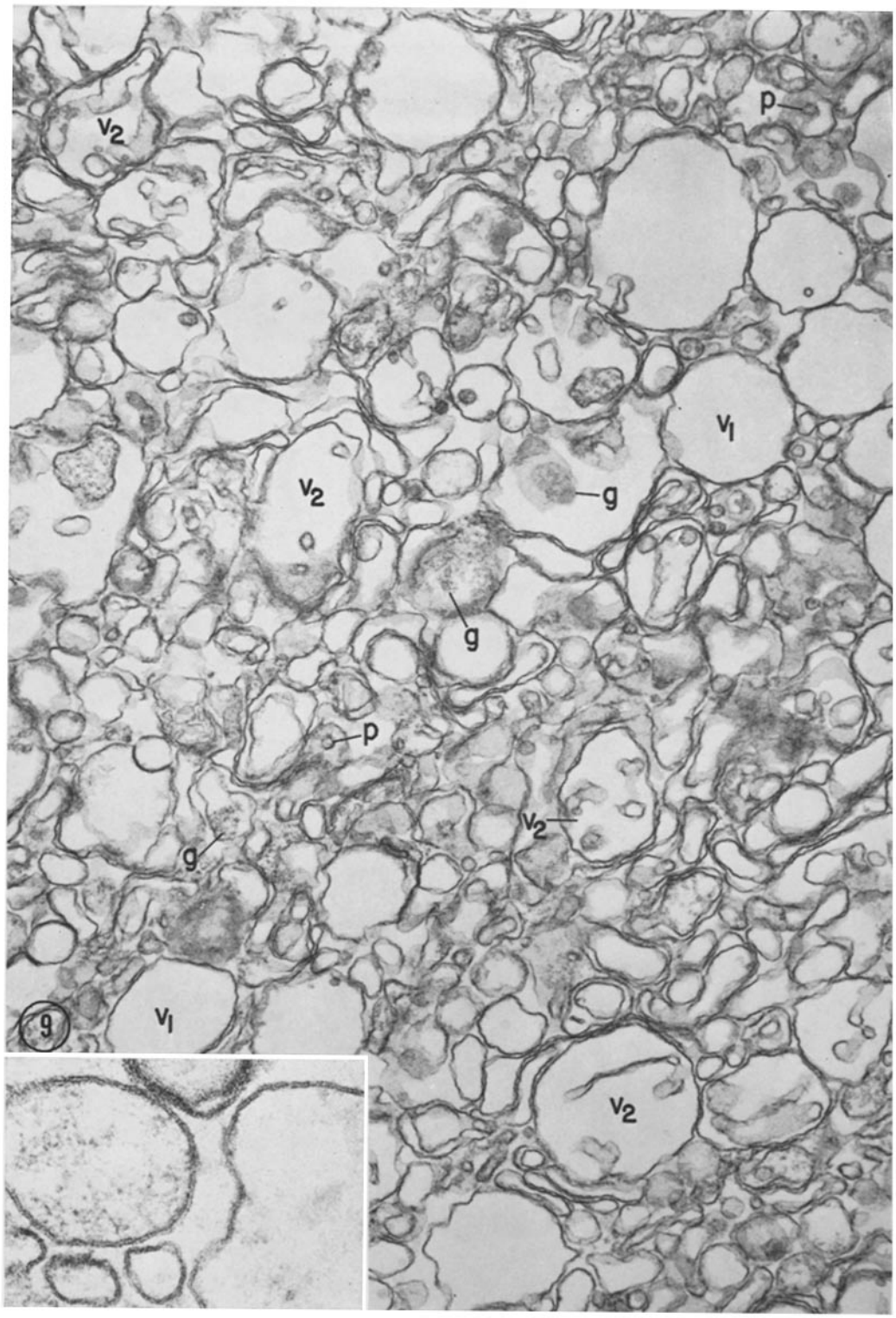

FIGURE 9 Nuclear envelope fraction isolated and processed for electron microscopy as in Fig. 8. At this higher magnification, many of the larger vesicles have tubules or small vesicles inside (v_2), while some of them appear empty (v_1). Grazing sections show that the membrane of some of these vesicles is covered by fine granules (g), possibly ribosomal remnants. There are no structures that can be reliably identified as nuclear pores, although a few suggestive images are encountered (p). The *inset* shows that the membrane of the vesicles has a typical layered structure. × 42,000; *inset*, × 150,000.

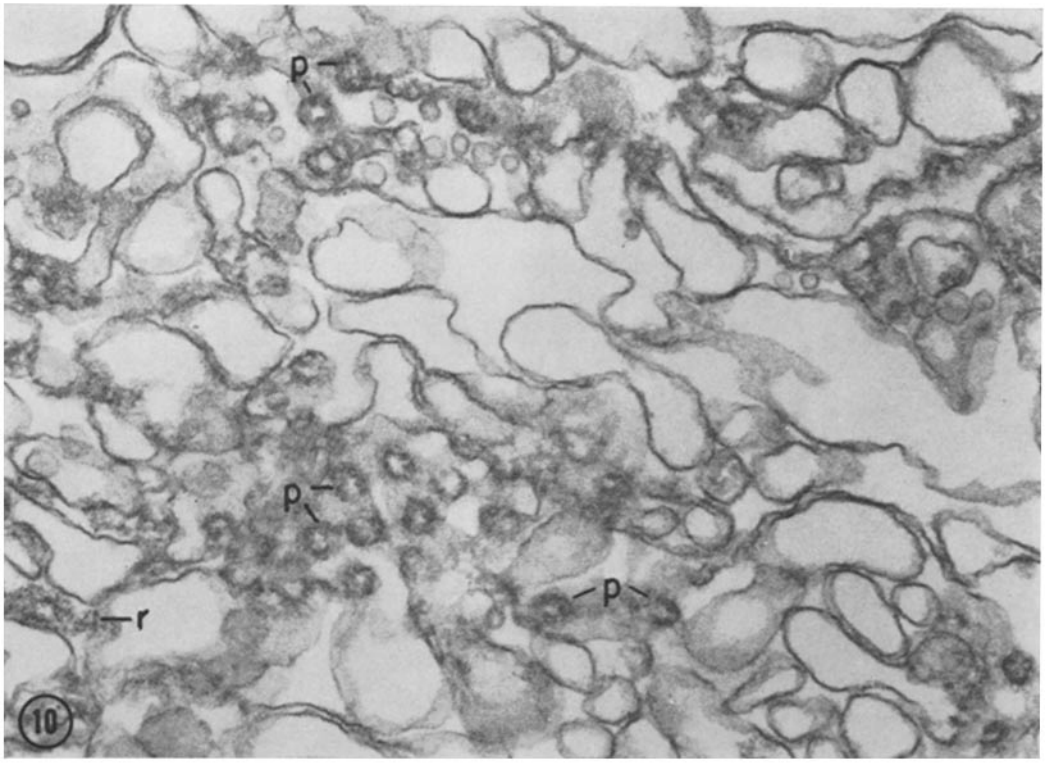

FIGURE 10 Nuclear envelope fraction prepared and isolated as in Figs. 8 and 9, but fixed in 1.6% buffered glutaraldehyde followed by 2% OsO_4 in water. The vesicles are less well preserved than in Fig. 9, but recognizable pores (*p*) can be seen on many grazing sections of vesicle membranes. Ribosomal remnants are marked *r*. × 72,000.

show graphically the interpretation of the majority (I) and minority (II) of pore appearances in the four views mentioned. The exact structure of the pore complex is still under discussion (cf. 26–30); the diagram in Fig. 4 is a convenient simplification that ignores details (such as annular granules [26]) which are not expected to appear in freeze-cleaved specimens.

B. Disruption of Nuclei by Monovalent or Divalent Cations

When isolated nuclei were suspended in increasing concentrations of KCl or $MgCl_2$, a dramatic increase in the viscosity of the suspensions and a concomitant decrease in their turbidity occurred above a concentration of 150–200 mM for $MgCl_2$ and 300 mM for KCl, probably due to the liberation of part of the DNA from its complexes with proteins.

Electron microscopic examination of the remaining structures in these viscous suspensions revealed striking differences between the two cations. In the case of $MgCl_2$ (Fig. 5), the nuclear envelope was frequently preserved as a "ghost" with much of the nuclear content extracted (including the dense chromatin underlying the inner membrane); whereas in the case of KCl (Fig. 6), the nuclear envelope was fragmented into small vesicles and large blocks of dense chromatin were still recognizable. Furthermore, the nucleoli appeared to be well preserved after $MgCl_2$, but were no longer detectable after KCl.

C. Isolation of Nuclear Membranes

The presence of well-preserved nuclear envelopes, largely freed from their previous associations with chromatin in media of high ionic strength, provided the rationale for the attempt to separate them from the other nuclear components. To this intent, nuclei suspended in high

concentrations of $MgCl_2$ and sucrose were loaded at the bottom of centrifuge tubes and the separation of the nuclear envelopes was achieved by floating them, in an appropriate centrifugal field, into a linear density gradient built above the load. After a short centrifugation a milky band could be seen in the gradient, with the load zone remaining only slightly turbid. Similar results were obtained when the nuclei were extracted with 0.5 M $CaCl_2$ or $MnCl_2$, instead of $MgCl_2$, but no further characterization of the fractions was performed. The band showed up as a peak in a recording at 440 nm (Fig. 7 A) with little absorbance left in the load zone of the tube. However, a recording at 260 nm (Fig. 7 B) showed, in addition to the peak corresponding to the milky band, a tail towards the loading zone and strong absorption in the latter, due to its high content in nucleic acids (see Table I). Refloatation of the band after its collection from a first gradient resulted in a symmetrical peak in the same position (Fig. 7 B, dotted line), the previously high A_{260} being now largely eliminated from the middle of the gradient and the load zone.

Among the variables involved in the procedure, we investigated the effects of centrifugation time and $MgCl_2$ concentration. Centrifugation for less than 2 hr (30 min, 1 hr) gave a smaller A_{260} peak in the same region of the gradient, whereas centrifugation for more than 2 hr (4 hr, 12 hr) resulted in progressive aggregation within the band without further increase of the peak. With $MgCl_2$ concentrations of 0.3 M, 0.5 M, and 0.7 M the band floated to slightly higher positions in the gradient corresponding to sucrose concentrations of 39%, 37%, and 34% and densities (i.e., sum of densities of sucrose and $MgCl_2$) of 1.169, 1.179, and 1.184, respectively (R. Aaronson, unpublished).

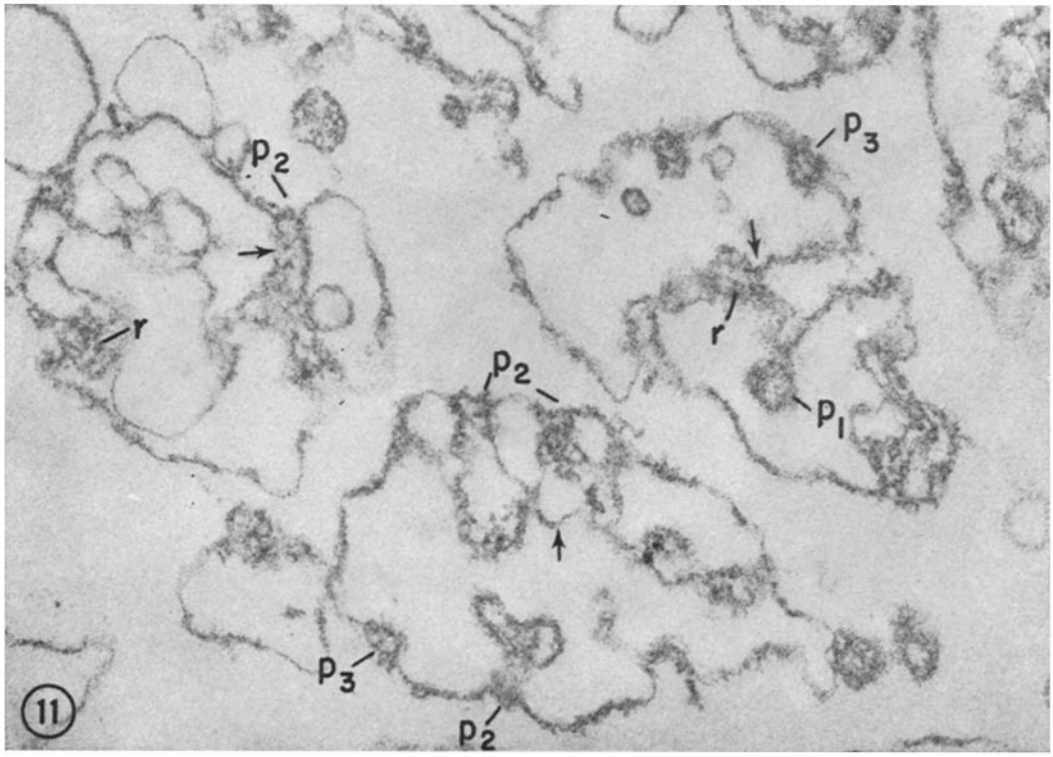

FIGURE 11 Nuclear envelope fraction prepared and isolated as in Fig. 8, but fixed in 1.8% glutaraldehyde in 0.5 $MgCl_2$. The preparation consists of vesicles of irregular profiles, some of which have enclosed channels (arrows) and smaller vesicles. Pores can be seen in full face view (p_1) and in normal section (p_2). Local membrane thickenings (p_3) could represent either pore complexes cut normally at the beginning of a channel or pore plugs left attached to a single membrane. Dense ribosomal aggregates are marked *r*. × 70,000.

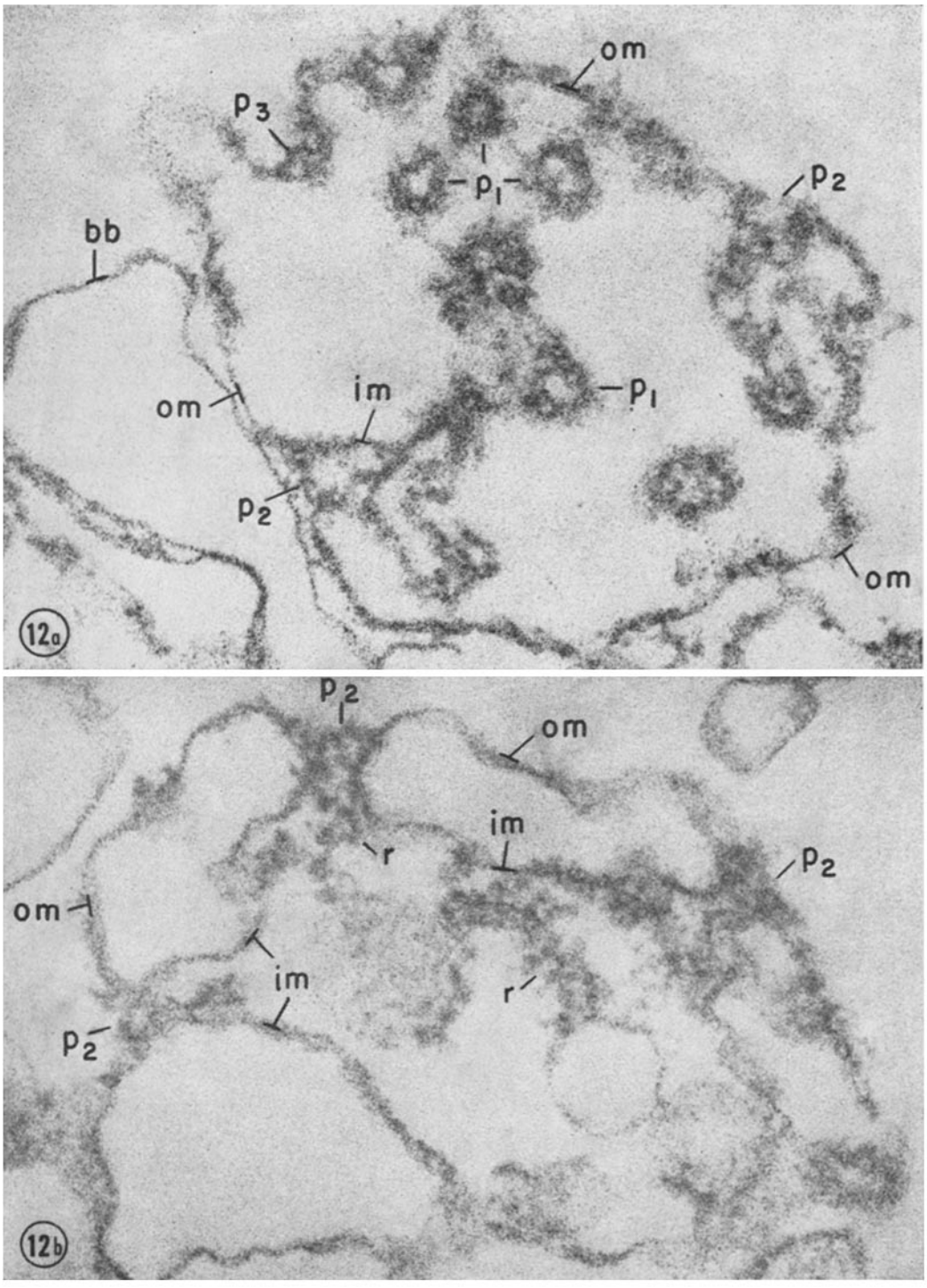

FIGURE 12 Nuclear envelope fraction prepared, isolated, and fixed as in Fig. 11. Higher magnification of vesicle similar to the ones in Fig. 11. The outer membrane is marked *om*; the inner membrane, which forms the enclosed channels, *im*. Numerous nuclear pores appear in full-face view (p_1), in normal section (p_2) at the beginning of the channels, or as local thickenings (p_3) attached to the outer membrane. The latter appearance may represent detached plugs or oblique sections through the beginning of channels. A pore-free bleb appears at *bb* in Fig. 12 *a*. Ribosomal remnants in the inner channels in Fig. 12 *b* are marked *r*. × 130,000.

If KCl was used instead of $MgCl_2$, a band could also be floated from the load, but centrifugation times of 10 hr and more were required until no further visible increase in the A_{260} peak was observed. Furthermore, there was frequently aggregated material in the zone below the band, with long streaks reaching into the load zone.

D. Morphological Characterization of the Banded Material

(1) Sectioned Specimens

In sections, the pelleted bands were found to consist of closed vesicles that varied in appearance according to the type of extraction and fixation.

(*a*) FRACTIONS PREPARED FROM $MGCL_2$ EXTRACTED NUCLEI: (i) When the pelleted bands were fixed in OsO_4 in hypotonic buffer, the fraction appeared as a tightly packed conglomerate of vesicles of varied size (from 100 to 3000 mμ in diameter) and shape with a relatively high proportion of spherical forms (Fig. 8). Most of the vesicles appeared to be bounded by a single, ~ 50 A thick membrane of the usual triple-layered structure (Fig. 9, inset), but in the larger ones there were tubular elements possibly representing remnants of a second, "inner" membrane (Figs. 8, 9). There were few or no flattened cisternae comparable in appearance to the envelope of isolated nuclei (cf. Figs. 2, 5), few and doubtful

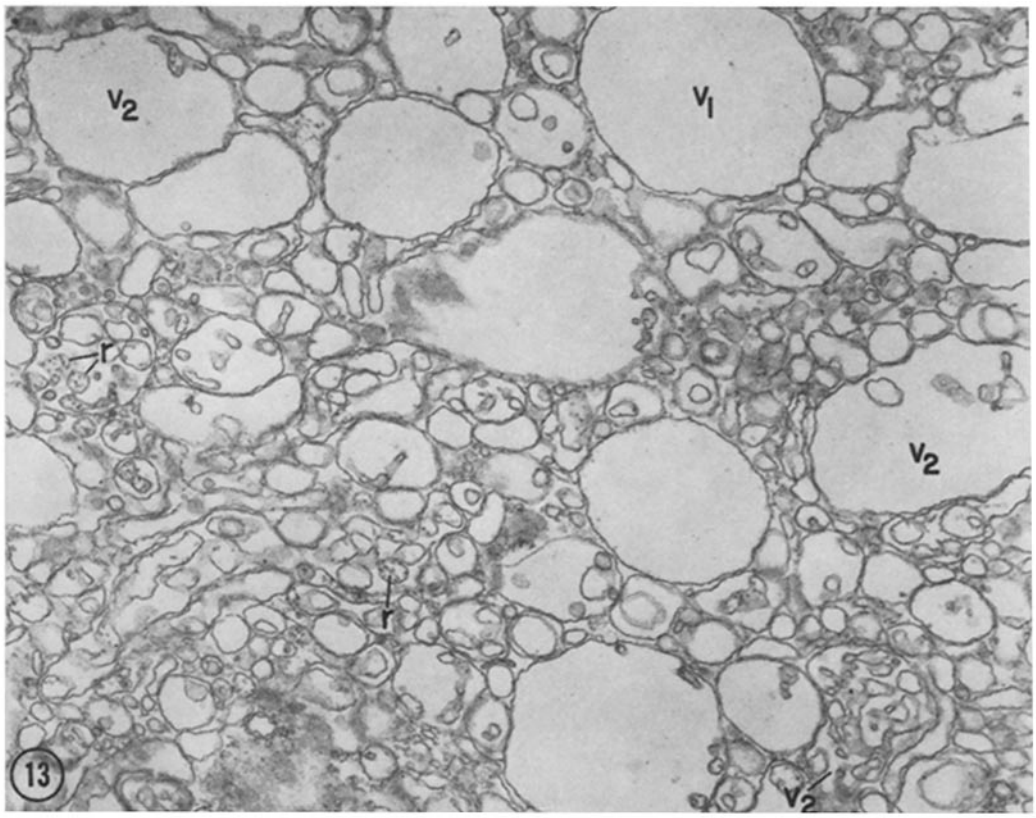

FIGURE 13 Nuclear envelope fraction prepared from nuclei extracted with 0.5 M KCl in 0.005 M $MgCl_2$-0.05 M Tris-HCl buffer, pH 7.5. The nuclear envelope membranes were isolated from the extract by floatation in a sucrose density gradient, as described under Methods. The ensuing band was diluted with the extraction medium and pelleted by centrifugation for 2 hr at 78,500 $g_{(avg)}$. The pellet was fixed in 2% OsO_4 in acetate Veronal buffer, pH 7.4. The fraction consists of packed vesicles of various sizes; some appear empty (v_1), others show enclosed channels (v_2) and smaller vesicles. The small particles (r) within these enclosed structures are probably ribosome remnants. Recognizable pores are absent. × 30,000.

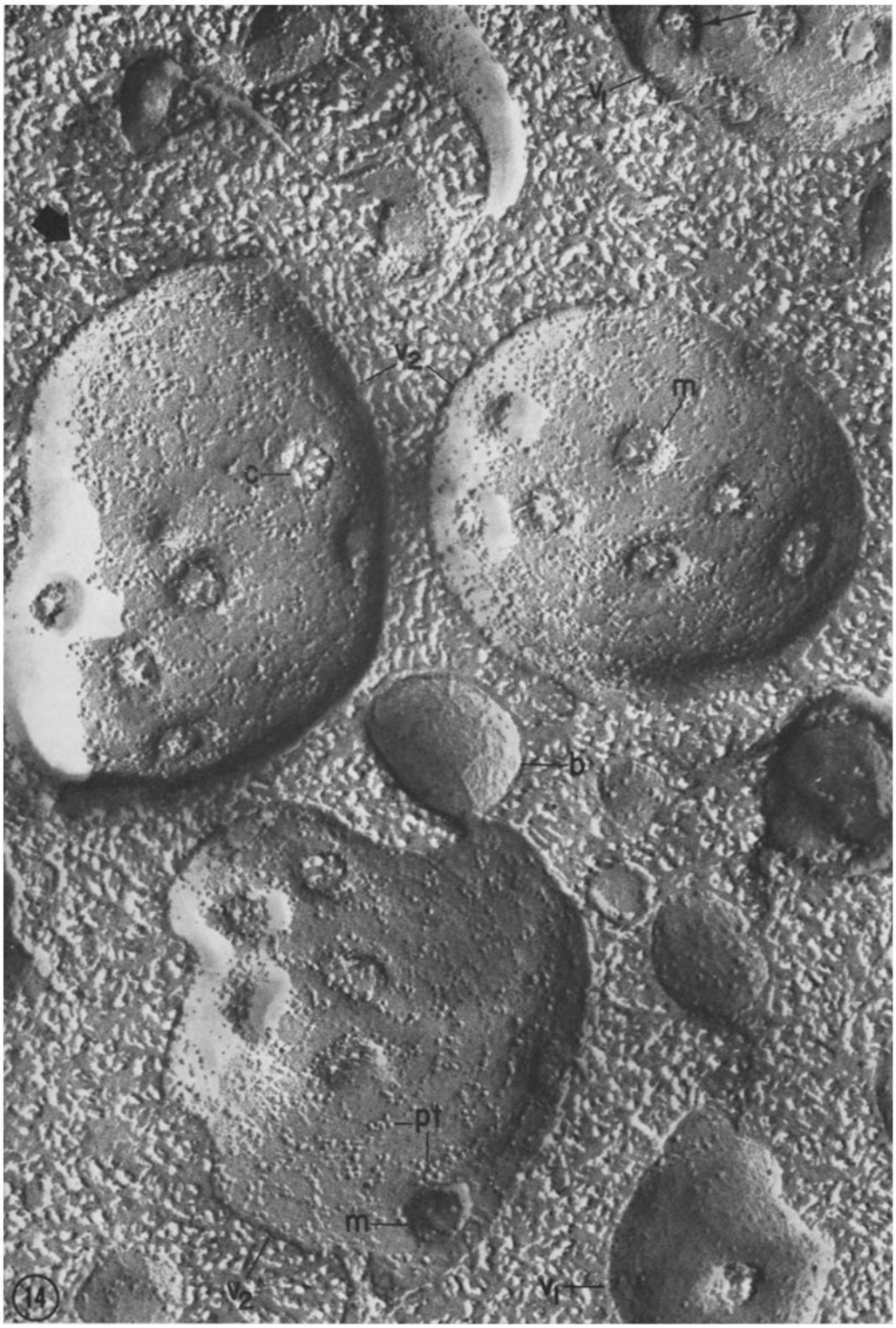

FIGURE 14 Nuclear envelope fraction prepared and isolated as for Fig. 8. Replica of freeze-cleaved specimen. The direction of the shadowing is indicated by the heavy arrow. Vesicles with convex surfaces (v_1) have depressed pores, some of which retain the appearance of circumvallate papillae (arrow). Vesicles with concave surfaces (v_2) have a large population of small particles frequently disposed in rows or clusters (*pt*) and numerous pores which appear as either craters (*c*) or mounds (*m*). A few apparently pore-free blebs (*b*) are scattered in the preparation. × 105,000.

images of pores either in normal or grazing sections, and few recognizable remnants of attached ribosomes.

(ii) After glutaraldehyde-OsO_4 fixation, the general appearance of the vesicles remained the same (except for the relatively frequent formation of myelin forms), but pore complexes $\sim$ 800 A in diameter with a slightly deformed but still recognizable annulus and occasionally with a central granule could be identified primarily in grazing sections (Fig. 2) of vesicles of all sizes.

(iii) In specimens fixed in 1.8% glutaraldehyde in the presence of 0.5 M $MgCl_2$, it became apparent that many of the forms described above were due to swelling before (or during) fixation under hypotonic conditions. In these specimens, many vesicles had two membranes connected with one another at the level of pores. The inner membrane frequently formed blebs in between the pores, and in extreme cases these blebs led to the appearance of a network of tubules anchored in the "outer" membrane of the vesicles at the pore level (Figs. 11, 12 *a*, *b*). Pore complexes could be recognized in normal as well as in grazing sections and in some instances they appeared to be associated with a single membrane (Fig. 11), usually the outer one, perhaps as a result of a pinching off of the inner membrane along the periphery of the pore. Irregular aggregates of dense particles, presumably ribosome remnants, occurred in the inner channels or in contact with the inner membrane (Fig. 12 *b*), an observation which suggests that, upon fragmentation, the envelope forms closed vesicles in which both membranes are involved, but in which their topography is inverted: the inner membrane of the envelope provides the outer membrane of the vesicles, whereas the outer membrane of the envelope forms the inner channels. The formation of the latter could be related to the tendency of this membrane to develop blebs on isolated nuclei. Notwithstanding their complicated geometry, most of these vesicles still appear to be limited by a continuous membrane (Figs. 11, 12 *a*) and, hence, are expected to behave like osmometers. Exposure to hypotonic media after isolation may lead, however, to pinching off or rupture of the inner channels, giving appearances of the type seen in Figs. 8–10.

(*b*) ENVELOPES PREPARED FROM KCL-EXTRACTED NUCLEI: When fixed in hypotonic OsO_4 solutions, the corresponding pellets were quite similar to those described above (Results, section D, 1, *a*, i) except that the membranes had lower density and that the small particles, most probably ribosomal remnants, were better defined and could be recognized within the membrane-bounded channels seen inside the large vacuoles (Fig. 13).

(2) Negatively Stained Specimens

The best results were obtained with ammonium molybdate and fresh, unfixed material obtained from $MgCl_2$-extracted nuclei. The vesicles of these preparations showed images of pore complexes with well-formed annuli and occasional central granules. Rather often the annuli appeared connected by membrane strands presumably formed at the expense of the inner membrane of envelopes prepared by the $MgCl_2$ procedure.

(3) Freeze-Cleaved Preparations

Freeze-cleaved preparations showed populations of vesicles of varied size (from 100 to 3000 mμ) and shape (from spherical sacs to flattened cisternae), the latter definitely in minority (Figs. 14, 15). Most of the vesicles were evenly covered by pores, some were only partly covered, and finally others had no pores at all. Since the original curvature of the envelope was lost and since most of the vesicles were spherical, a distinction between inner and outer membrane of the envelope was not possible. Convex surfaces showed depressed pore images comparable to those seen on the faces A and C of the envelope *in situ* (Fig. 3), except that depressions with a flat bottom were more numerous. On concave surfaces the pores appeared as craters or mounds like on the faces B and D of the envelope *in situ* (Fig. 3), except that the frequency of mounds was higher. The large majority of concave surfaces showed a single line of membrane fracture at their periphery (Fig. 14), not two as in Fig. 3 *i*, which clearly indicates that they belonged to spherical vesicles and not to flattened sacs. In the few instances in which the fracture cleaved the membrane on both sides of a flattened vesicle (Fig. 15), the appearance of the pores on the various cleavage faces seemed to be the same as in the case of spherical vesicles. The variety of appearances recorded suggests that during the preparation procedure, the envelope undergoes some blebbing—which accounts for the pore-free areas—and extensive fragmentation, that the ensuing vesicles swell, and that beyond a certain degree of swelling the pore complex is detached from one side of the vesicle and remains

attached only to the other on which it can be recognized either as a mound or a circumvallate papilla. Such overextended vesicles are no longer expected to behave like osmometers since the continuity of their single membrane is now interrupted by pores. But they do not collapse, presumably because their walls remain fixed in a distended position. Only rarely are images of membrane-bounded channels found inside the vesicles, possibly connecting the two sides of a dismantled pore, like in sectioned material fixed under hypertonic conditions (Fig. 15).

As a result of this examination by a variety of procedures we can conclude that: (*a*) the banded material consists mostly of closed, osmotically active vesicles; (*b*) many of these vesicles still have pores and pore complexes which clearly establish their derivation from nuclear envelopes; (*c*) artifacts incurred during the preparation of the fraction include fragmentation, blebbing, and disorganization of ribosomes; and (*d*) artifacts incurred during the processing of the fraction for electron microscopy include swelling, leading in extreme cases to the pore complexes remaining attached to a single membrane, and partial or complete extraction of the pore complexes during

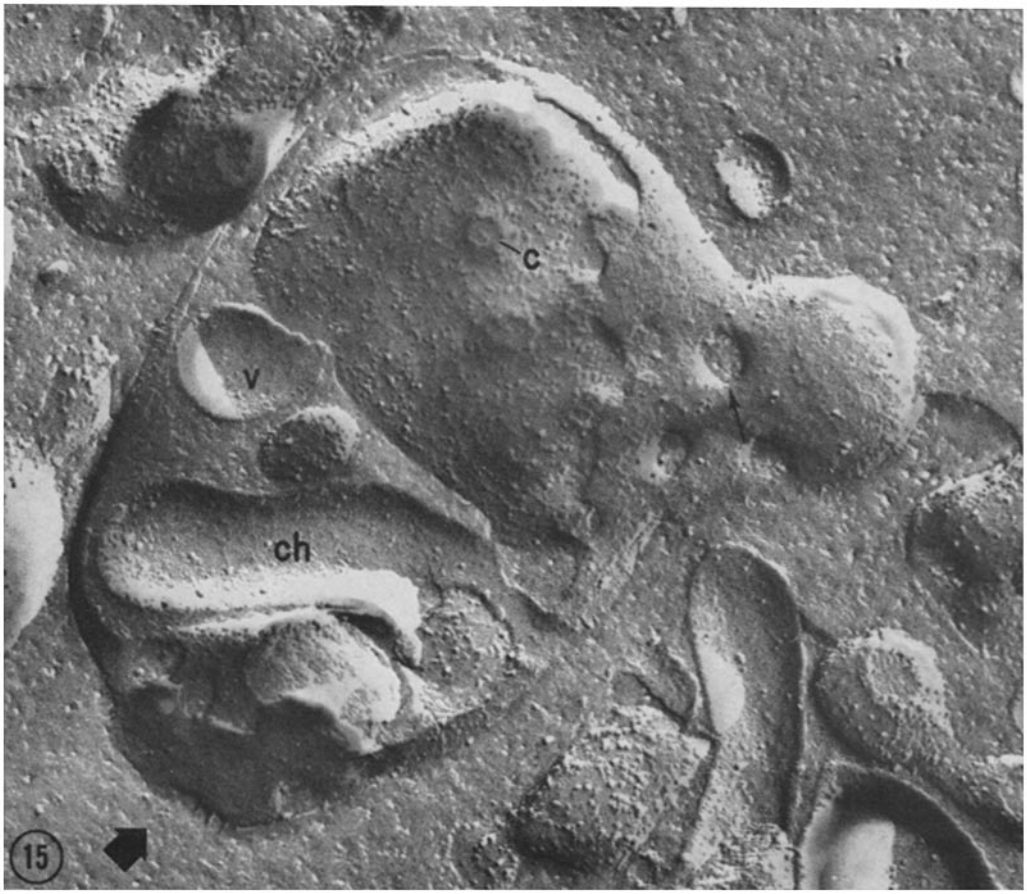

FIGURE 15 Nuclear envelope fraction prepared and isolated as in Fig. 8. Replica of freeze-cleaved specimen. The heavy arrow indicates the direction of shadowing. The fracture goes through a large vesicle derived from a nuclear envelope. In the upper part, where the vesicle is flattened, the fracture cleaves both membranes. One of the cleavage faces shows depressed pores with flat bottoms (arrow); the other, craters (*c*) and small particles. The lower half of the vesicles has a complicated geometry with a few enclosed small vesicles (*v*) and a long channel (*ch*) starting from the surface and reaching far inside. × 90,000.

fixation, especially during fixation in OsO_4 solutions.

E. Composition of Isolated Nuclear Envelopes

The distribution of PLP, protein, RNA, and DNA in the gradient was determined in four separate experiments. The balance sheet of one experiment is given in detail in Table I. The data relevant to recovery and composition of the nuclear envelopes were compiled from four experiments in Tables II and III, respectively.

On the assumption that all nuclear PLP is located in the membranes of the nuclear envelope, it can be seen from Table II that 74% of these membranes were floated from the load zone into the gradient, with most of them concentrated in a narrow zone. Coincident with the PLP peak was a peak of protein and RNA, but not of DNA (Table I). Only 1% of the latter, but 24% of the protein and 12% of the RNA floated from the load zone into the gradient (Table II). Not all of this protein and RNA is part of the nuclear membranes. Some of it was clearly pulled along and subsequently lost as the membrane moved from the load zone through the lower part of the gradient. This is evident from the lower PLP:protein and PLP:RNA ratios in the fractions between the PLP peak and the load zone (Table I), i.e., from the proportionately higher recovery of protein and RNA in relation to PLP from the combined fractions above the load zone rather than from the PLP peak alone (Table II, line 1 vs. 2). The unusually high protein:PLP ratio in the first two fractions is probably due to residual foam (see Methods) which floated to the top when the continuous sucrose density gradient was generated over the load zone. Electron microscopy did not reveal organized membranes in this part of the gradient. Taking the composition of the PLP peak fraction (tube 4, Table III) as representative for the composition of the nuclear envelope, one can calculate that it contains 22% of the nuclear protein, 9% of the nuclear RNA, and 0.4% of the nuclear DNA.

TABLE II

Recovery (%) of Phospholipid, Protein, RNA, and DNA in Gradient Fractions

	Gradient fractions	PLP	Protein	RNA	DNA
PLP Peak	3–6	58 ± 2	12 ± 2	6 ± 1	0.6 ± 0.3
Floated fraction	1–9	74 ± 4	24 ± 4	12 ± 2	1.0 ± 0.5
Load zone + pellet	10–12	26 ± 1	76 ± 7	88 ± 2	99 ± 1

Recovery from 12 tubes and pellet (see Table I) was set to equal 100%. Values are means from four experiments ± SE of the means.

TABLE III

Composition (%) of Nuclei, Nuclear Membrane Fractions, and Rough Microsomes

	PLP	Protein	RNA	DNA
Nuclei	4.4 ± 0.5	63 ± 3	6.5 ± 0.9	26 ± 2
PLP peak (tube 4)	23 ± 2	73 ± 4	3 ± 1	0.6 ± 0.2
PLP peak (tubes 3–6)	17 ± 2	78 ± 5	4 ± 2	0.6 ± 0.4
Rough microsomes (tubes 3–6)	26	61	13	—

Phospholipids, proteins, RNA, and DNA were assumed to be 100% of the mass. Values for nuclei and the two PLP peak fractions (see Table I and Fig. 7) are means from four experiments ± SE of the means. Values for rough microsomes are from one experiment.

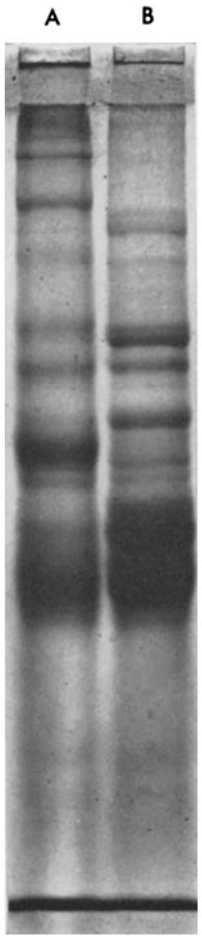

FIGURE 16 Electropherogram of the polypeptides of (A) the nuclear envelope fraction (tube 3–6), and (B) rough microsomes (tube 3–6) in a 7.5% acrylamide-SDS gel. For further details see Methods and Table III.

The composition of the nuclear envelope was clearly different from that of rough microsomes exposed to identical preparatory conditions. The nuclear envelope had more protein, less phospholipids, and considerably less RNA than rough microsomes (Table III).

In addition to these differences in gross chemical composition, there were also differences in polypeptide components between the two types of membranes. SDS-gel electrophoresis (Fig. 16) showed several bands in nuclear envelopes which were entirely absent in rough microsomes or vice versa. Both preparations, however, had bands in common. The nuclear envelope fraction described has not yet been characterized enzymatically. Enzyme assays that will show characteristic enzymatic activities, if any, as well as the extent of contamination by other cellular membranes (mitochondria, plasmalemma) remain to be carried out in future work. On the basis of the morphological evidence already obtained, the contamination appears to be of rather limited importance.

DISCUSSION

The fraction isolated by our procedure consists of vesicles primarily derived from the nuclear envelope as shown by the pores and pore complexes which they retain throughout the preparation procedure and which can be reliably identified in freeze-cleaved preparations. Results obtained by a combination of preparative procedures for electron microscopy indicate that both membranes of the envelope are involved in the formation of these vesicles, but their topography is inverted: the inner membrane of the envelope apparently becoming the outer membrane of the vesicles.

By comparison with published procedures, our method has the following advantages: (*a*) It gives a higher membrane yield: 74% of the PLP of the treated nuclear fraction is floated in the gradient and 55–60% is recovered in the membrane band. (*b*) It has a lower content of DNA than most other fractions (2, 4), including those prepared by DNase treatment (4). There is in the literature a single fraction which is reported to contain no DNA (1). (*c*) It requires less time ($\sim$ 3 hr starting from isolated nuclei, and 6 hr starting from fresh tissue) and fewer manipulations than all available procedures. (*d*) It avoids the use of enzymes to degrade nuclear macromolecules and of physical means to disrupt nuclear structures before the extraction of the nuclear content. In fact it shows that these steps are not necessary.

In other respects, primarily protein content, our fraction is comparable to already available preparations. It has, for instance, a lower PLP: protein ratio than other cellular membranes. In our case, the ratio is lower than that found in microsomes treated with 0.5 M $MgCl_2$, although the latter contain a higher proportion of attached ribosomes than the envelope. The high protein content may reflect the presence of a large population of pore complexes still associated with the membranes recovered in the fraction.

Our findings do not support Agutter's assump-

tion (31), that the presence of a relatively large amount of DNA ($\sim$ 8% of the calculated dry weight of his nuclear envelope preparation) is required for the structural integrity of the envelope and its pore complexes. The tendency of the envelope to break down into small vesicles in KCl solutions has also been recorded (31), and published observations indicate that Mg^{2+} is required for the preservation of pore complexes (26), while K^+ and Na^+ above certain concentrations cause the removal or extraction of the pore plugs (26, 31). Our findings are in general agreement with these observations, but a detailed comparison of the data is not possible because media of greatly different ionic strength have been used in the references mentioned (26, 30, 31) and in our work.

It is hoped that this preparation will prove useful as a starting material for the isolation and characterization of its RNA and proteins, especially of these proteins which appear to be absent from a rough microsomal fraction isolated from the same tissue.

For the moment, we would like to point out that it proved possible to dismantle the entire structure of isolated nuclei by extracting them with media of high ionic strength, the extraction with $MgCl_2$ at high concentrations being particularly effective. These results strongly suggest that the organization of the nucleus, including the association of the peripheral chromatin with the nuclear envelope, depends primarily on ionic interactions. If so, a comprehensive subfractionation of the nucleus into structures and macromolecular complexes of physiological significance could be attempted by using a series of appropriately high concentrations of divalent cations.

Mr. Roland Blischke's expert assistance with the freeze-etch work is gratefully acknowledged.

Received for publication 7 February 1972, and in revised form 5 June 1972.

REFERENCES

1. KASHNIG, D., and C. KASPER. 1969. Isolation, morphology and composition of the nuclear membrane from rat liver. *J. Biol. Chem.* **244:** 3786.
2. FRANKE, W., B. DEUMLING, B. ERMEN, E. JARASCH, and H. KLEINIG. 1970. Nuclear membranes from mammalian liver. I. Isolation procedure and general characterization. *J. Cell Biol.* **46:** 379.
3. UEDA, K., T. MATSUURA, and N. DATE. 1969. The occurrence of cytochromes in the membranous structures of calf thymus nuclei. *Biochem. Biophys. Res. Commun.* **34:**322.
4. BEREZNEY, R., L. FUNK, and F. CRANE. 1970. The isolation of nuclear membrane from a large scale preparation of bovine liver nuclei. *Biochim. Biophys. Acta.* **203:**531.
5. ZBARSKY, J., K. PEREVOSHCHIKOVA, L. DELEKTORSKAYA, and V. DELEKTROSKY. 1969. Isolation and biochemical characteristics of the nuclear envelope. *Nature (Lond.).* **221:**257.
6. BLOBEL, G., and V. R. POTTER. 1966. Nuclei from rat liver: isolation method that combines purity with high yield. *Science (Wash. D. C.).* **154:** 1662.
7. BLOBEL, G., and D. SABATINI. 1970. Controlled proteolysis of nascent polypeptides in rat liver cell fractions. I. Location of the polypeptides within ribosomes. *J. Cell Biol.* **45:**130.
8. SABATINI, D., and G. BLOBEL. 1970. Controlled proteolysis of nascent polypeptides in rat liver cell fractions. II. Location of the polypeptides in rough microsomes. *J. Cell Biol.* **45:**146.
9. LOWRY, O. H., N. J. ROSEBROUGH, A. L. FARR, and R. J. RANDALL. 1951. Protein measurement with the Folin phenol reagent. *J. Biol. Chem.* **193:**265.
10. FOLCH, J., M. LEES, and G. STANLEY. 1957. A simple method for the isolation and purification of total lipids from animal tissues. *J. Biol. Chem.* **226:**497.
11. AMES, B., and D. DUBIN. 1960. The role of polyamines in the neutralization of bacteriophage deoxyribonucleic acid. *J. Biol. Chem.* **235:**769.
12. BLOBEL, G., and V. R. POTTER. 1968. Distribution of radioactivity between the acid-soluble pool and the pools of RNA in the nuclear nonsedimentable and ribosome fractions of rat liver after a single injection of labeled orotic acid. *Biochim. Biophys. Acta.* **166:**48.
13. BURTON, K., and PETERSON, G. B. 1957. The quantitative distribution of pyrimidine nucleotides in calf thymus deoxyribonucleic acid. *Biochim Biophys. Acta.* **26:**667.
14. MAIZEL, J. V. 1969. Acrylamide gel electrophoresis of proteins and nucleic acids. *In* Fundamental Techniques in Virology. K. Habel and N. P. Salzman, editors. Academic Press Inc., New York. 334.
15. LUFT, G. H. 1961. Improvements in epoxy embedding methods. *J. Biophys. Biochem. Cytol.* **9:** 409.
16. FARQUHAR, M. G., and G. E. PALADE. 1965. Cell junctions in amphibian skin. *J. Cell Biol.* **26:** 263.

17. WATSON, M. L. 1958. Staining of tissue sections for electron microscopy with heavy metals. *J. Biochem. Biophys. Cytol.* **4**:475.
18. VENABLE, J., and R. COGGESHALL. 1965. A simple lead citrate stain for use in electron microscopy. *J. Cell Biol.* **25**:407.
19. MOOR, H., K. MÜHLETHALER, H. WALDNER, and A. FREY-WISSLING. 1961. A new freezing ultramicrotome. *J. Biophys. Biochem. Cytol.* **10**:1.
20. MOOR, H., and K. MÜHLETHALER. 1963. Fine structure of frozen-etched yeast cells. *J. Cell Biol.* **17**:609.
21. BRANTON, D. 1966. Fracture faces of frozen membranes. *Proc. Natl. Acad. Sci. U. S. A.* **55**:1048.
22. MAGGIO, R., P. SIEKEVITZ, and G. E. PALADE. 1963. Studies on isolated nuclei. I. Isolation and chemical characterization of a nuclear fraction from guinea pig liver. *J. Cell Biol.* **18**: 267.
23. BRANTON, D., and R. B. PARK. 1967. Subunits in chloroplast lamellae. *J. Ultrastruct. Res.* **19**:283.
24. MAUL, G. G., J. W. PRICE, and M. W. LIERMAN. 1971. Formation and distribution of nuclear pores in interphase. *J. Cell Biol.* **51**:405.
25. MAUL, G. G. 1971. On the octogonality of the nuclear pore complex. *J. Cell Biol.* **51**:558.
26. FRANKE, W. W. 1970. On the universality of the nuclear pore complex structure. *Z. Zellforsch. Mikrosk. Anat.* **105**:405.
27. ABELSON, H. T., and G. H. SMITH. 1970. Nuclear pores: the pore-annulus relationship in thin sections. *J. Ultrastruct. Res.* **30**:558.
28. VIVIER, E. 1967. Observations ultrastructurales sur l'envelope nucléaire et ses "pores" chez les sporozoaires. *J. Microsc. (Paris).* **6**:371.
29. YOO, B. Y., and S. T. BAYLAY. 1967. The structure of pores in isolated pea nuclei. *J. Ultrastruct. Res.* **18**:651.
30. GALL, J. G. 1967. Octogonal nuclear pores. *J. Cell Biol.* **32**:391.
31. AGUTTER, P. S. 1972. The isolation of the envelopes of rat liver nuclei. *Biochim. Biophys. Acta.* **255**:397.